JOM Journal of Optical Microsystems

RESEARCH PAPER

Unraveling the role of plasmonics in gold nanoparticle-integrated tapered fiber platforms for sensing applications

Debanita Das,[a,b,c] Anuj Kumar Singh,[a] Kishor Kumar Mandal,[a] Alison May Funston,[b,*] and Anshuman Kumar[a,*]

[a]Indian Institute of Technology Bombay, Laboratory of Optics of Quantum Materials, Department of Physics, Mumbai, Maharashtra, India

[b]Monash University, Department of Chemistry, Clayton, Victoria, Australia

[c]IITB-Monash Research Academy, Indian Institute of Technology Bombay, Mumbai, Maharashtra, India

ABSTRACT. We demonstrate the use of cost-effective tapered telecommunication fiber in refractive index-based sensing when operated in the visible range of wavelength. To fabricate the tapered fiber, a two-step chemical-etching method is adopted. The two-step etching method is quintessential in overcoming issues such as the uncontrollable etching of Ge-doped silica fibers by hydrofluoric acid. The work details the optimization of the etching process. The tapered fiber is then chemically treated to immobilize gold nanoparticles on it. Finally, the performance of the proposed Au-immobilized tapered fiber sensor probe is studied when excited with visible light. Different concentrations of sucrose are used to detect the refractive index sensitivity. Performance parameters such as sensitivity, full-width half maximum, the figure of merit, and quality factor are determined for the sensor probe.

Keywords: sensor; tapered fiber; refractive index sensing; intensity-modulated; wavelength-modulated; localized surface plasmon

Paper 24007SS received Mar. 6, 2024; revised Dec. 2, 2024; accepted Dec. 3, 2024; published Dec. 14, 2024.

1 Introduction

Since the 1970s, optical fibers have played a major role in modern telecommunications due to their low attenuation in long-distance light transmission.[1] In addition to their wide application in communication, significant efforts have been invested in exploring the potential of optical fibers in the field of sensing. An optical fiber is a device that uses light propagation to interact with the measurand in the surrounding medium. Parameters such as intensity, phase, polarization, and wavelength of the transmitted light can be modified by local environmental factors which, in turn, can convert the measurands to measurable and quantifiable optical signals.[2] Currently, using different parameters, optical fibers can detect a change in the refractive index of the surrounding medium; for instance, they can detect the change in temperature,[3,4] strain,[3] pollutants,[5,6] gases,[7,8] and biomolecules.[9–13] Fiber optic sensors offer several advantages such as high stability, low weight, compact size and electromagnetic protection, flexibility, and electrical passivity with the measurand.[14]

Given the current demand for sensing particles at the nanometer scale, conventional fibers face a few limitations. For instance, the limited access to the evanescent field in conventional

*Address all correspondence to Anshuman Kumar, anshuman.kumar@iitb.ac.in; Alison May Funston, alison.funston@monash.edu

optical fibers results in inefficient light-matter interactions. This, in turn, results in poor sensitivity of the analyte. This drawback can be addressed by decreasing the diameter of the fiber that facilitates efficient access to the evanescent field due to the span of the field in the outer boundary. In addition, the reduced diameter fiber experiences stronger mode confinement in the localized tapered area[2] which enables the detection of small biomolecules or chemical particles.

The interaction between the measurand and light propagation can be detected in one of the following domains: intensity, phase, wavelength, or polarization state. The intensity modulation of a tapered optical fiber demands strong interaction between the evanescent field and the measurand. Exhibiting such a large evanescent field fraction requires that the diameter of the optical fiber be in the sub-wavelength range. However, such fibers are extremely fragile and have poor mechanical stability. To address this, it is essential to develop comparatively large and easily manageable diameters. However, large diameters of optical fibers generate smaller evanescent fields that are relative to the fiber of a sub-wavelength diameter; this results in poor interaction between the measurand and the evanescent light and in turn, poor sensitivity of the sensor. A tradeoff between stability and sensitivity can be achieved by integrating tapered fibers with strong resonances such as those that induce localized surface plasmon resonances (LSPR). The evanescent field coupled with deposited plasmonic nanoparticles excites the LSPR that is confined in the conductive-metal nanoparticles. The resonance frequency is found to be strongly dependent on the particles' shape, size, composition, and dielectric properties of the surrounding medium.[15,16] When the excitation wavelength that is coupled with the metal nanoparticle resonates with the collective oscillation of electrons in the noble metal, the nanoparticle can both absorb and scatter light around its geometric cross-section.[17] Owing to the higher intensities and shorter field decay distances in LSPRs than in the evanescent fields in tapered fibers, a stronger coupling of a biomolecule with light is possible; this modulates the properties of light and the LSPR. The presence of different dielectric constant media around the metal induces a change in the evanescent field distribution around the fiber and the metal. The modulation of light properties in terms of absorbance variation or spectral shift of LSPR can be monitored in real time through transmission or reflection methodologies.

The mass production of telecom fibers for the telecommunication industry, results in reduced cost of the fibers as compared to the visible fibers. The widespread use of these fibers also makes it readily available. The primary use of these fibers in the telecom industry also renders it to be robust. Thereby, ensuring reliable performance in the harsh environment. On the other hand, label-free detection without causing any damage to biomolecules can be easily realized with visible light. The limited penetration depth of visible light can be improved with its interaction with plasmonic material. Therefore, integrating cost-effective telecom fiber with visible light can leverage the accessibility of the existing sensing system.

Reduction in fiber diameter can be realized using a chemical etching method. However, such a core-cladding removal process introduces surface roughness and exhibits poor control over the diameter of the fiber section. This paper explored a two-step etching method to overcome these issues on a single-mode fiber (SMF). The reduced-diameter fiber was chemically treated for gold nanoparticle deposition. A commercial sucrose solution with varying concentrations was used to measure the change in the refractive index in the surroundings. The model experiment is demonstrated systematically.

2 Materials and Methods

2.1 Materials

Forty-nine percent to 50% of concentrated hydrofluoric acid (HF), concentrated sulphuric acid (H_2SO_4), and hydrogen peroxide (H_2O_2) were used as is. Mili-Q water, (3-mercaptopropyl)trimethoxysilane) (MPTMS), chloroauric acid, trisodium citrate, and molecular sieves were obtained from Sigma Aldrich. Single-mode G.652 (SMF-28) telecommunication optical fiber with core and cladding diameters of 9 and 125 μm, respectively, was employed. A supercontinuum laser was used as a light source and spectra were collected using an ANDOR spectrometer, two 630 nm $\pm$ 50 nm splitters with a 90:10 split ratio (Thorlabs, Newton, United States) were employed for the measurements. Two mirrors, one lens, and one fiber collimator from Thorlabs were used to design a free-space coupling setup.

2.2 Preparation of Tapered Fibers Using Hydrofluoric Acid

The polymer jacket was removed from a bare fiber using a stripper. The fiber was then cleaned in acetone and isopropyl alcohol (IPA) and stabilized on glass slides using transparent adhesive tape. A combination of 30% and 24% HF was used to taper the fiber. The process duration was varied, and the diameter was checked under an optical microscope. The HF concentration was optimized to obtain the minimum diameter of the SMF. The optimization data are shown in Fig. 1.

2.3 Synthesis of Au Nanoparticles

Gold nanoparticles were prepared and optimized using the Turkevich method.[18] A 0.1 g of gold chloride was dissolved in 500 ml of distilled water to obtain 1 mM of gold chloride solution. A 0.5 g of trisodium citrate dihydrate (TNaC) was dissolved in 50 mL water to obtain a 1% solution of TNaC. A 20 ml of 1 mM gold chloride solution was added to a cleaned conical flask and heated to 120°C; the solution was then brought to a boil. When the solution began to boil, the temperature was reduced to 100°C to reduce the loss of the solution through evaporation. To the rapidly stirred boiling solution, 2 ml of TNaC was quickly added. After 10 to 15 min, the solution turned ruby red, signaling the formation of gold nanoparticles.

2.4 Preparation of the Sensor Probe

The optical fiber was ultrasonically cleaned with DI water, acetone, and IPA. The SMFs in this experiment were treated with piranha solution (preparation: 3 mL of H_2O_2 was slowly added to 7 mL of H_2SO_4) for 30 min to form surface silanol sites and to render the surface hydrophilic.[19,20] The fibers were then thoroughly washed with DI water until the pH turned neutral. Maintaining the pH was found to be important for proper gold immobilization, failing which, the gold solution turned unstable and formed agglomerates. The silanol-activated fiber probes were then heated to remove adsorbed water from the surface. This step is important because MPTMS tends to polymerize in the presence of water. Previous work[21] has suggested heating the fiber probes at 110°C for 60 min; however, in this work, the fiber system was heated at a temperature below 60°C because that is the temperature at which the transparent adhesive tape, which was used to stabilize the fiber probes on glass slides, melts.

Thereafter, the fiber probes were dipped in 1% of an MPTMS solution which was prepared by mixing 250 μL of MPTMS in 25 mL of dry ethanol for 12 h; the ethanol was dried by soaking

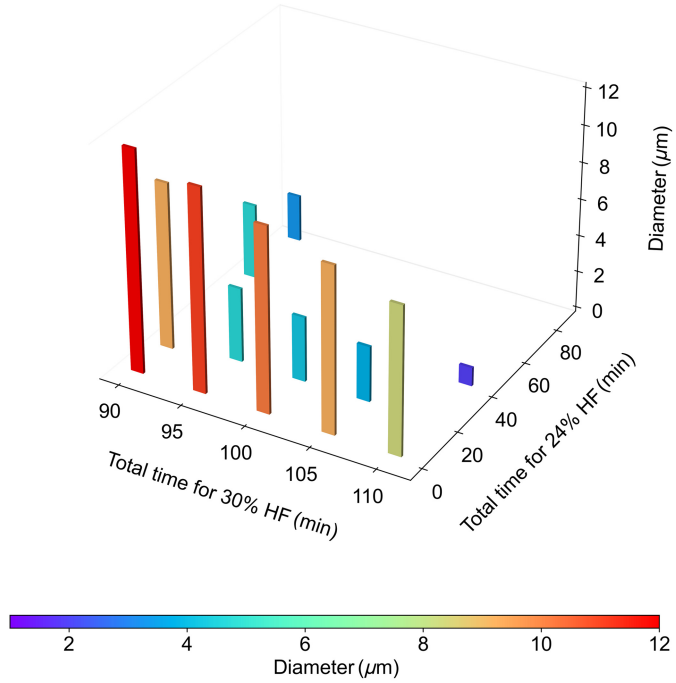

Fig. 1 Optimization curve for a combination of 30% and 24% of HF.

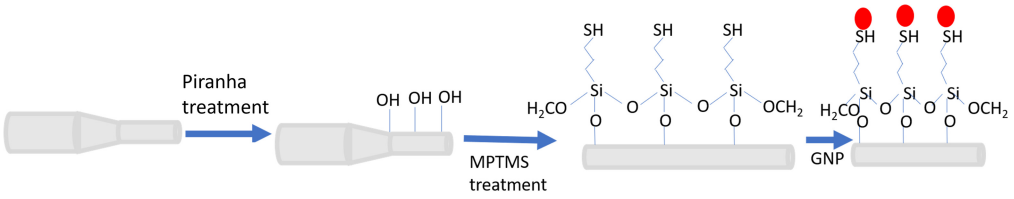

Fig. 2 The chemical reaction on the fiber when dipped in 1% of MPTMS.

it in molecular sieves for 72 h. We performed this process in a desiccator, which aided the formation of a monolayer of Au nanoparticles. An alternative is to heat the MPTMS solution at 78°C while soaking the probes. The fiber probes were then rinsed thoroughly with ethanol to remove any loosely bound silane. Following this, the fiber probes were dried in a nitrogen environment. The thiol-functionalized SMF was then immersed in the prepared gold nanoparticle solution and set aside for 48 h. The sulfur group in MPTMS is covalently attached to the AuNP. The chemical process of immobilizing AuNPs on tapered SMF has been shown in Fig. 2.

2.5 Optical Experiment Set-up

The SMF optical fiber was cleaved to obtain a flat end face that was perpendicular to the longitudinal axis of the fiber. Then, the fiber was fused with SMF using a fiber optic fusion splicer. In this device, an electric arc is used to melt the two ends of the optical fibers together at their end faces to obtain a single long fiber. The experimental setup for refractive index sensing is shown in Fig 3. Two 630 nm single-mode splitters were used to obtain the reflectance spectra. A supercontinuum laser was used light source. Free-space coupling setup was designed for this experiment. Light from the source was coupled to the fiber collimator using two mirrors and one lens. The first splitter was used to monitor the power input to the tapered fiber. The second splitter was used to couple light into the fiber probe. The tapered fiber was connected to the input end of the second splitter, the output from the first splitter was connected to the tap output end of the splitter, and the signal output end was connected to the ANDOR spectrometer, which provided an intensity signal from the functionalized microfibers.

3 Results and Discussions

3.1 Preparation of Tapered Fibers Using HF

Due to the fast etch rate of the Ge-doped silica core, it can be difficult to control the etch rate. In such a case, using diluted HF can slow down the etch rate. However, the process of etching takes excessive time because the cladding material above the core etches at a substantially slower rate

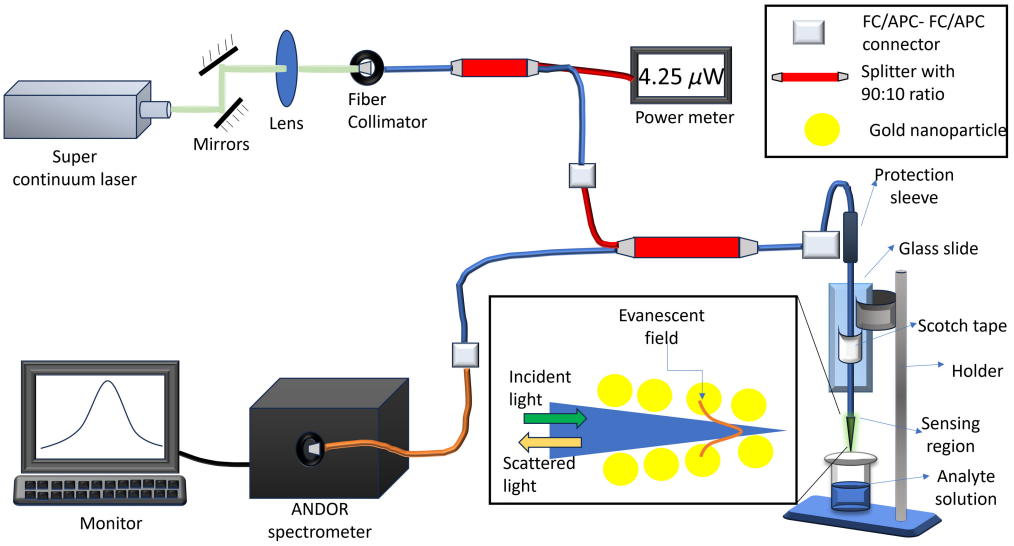

Fig. 3 Optical set-up for measurement.

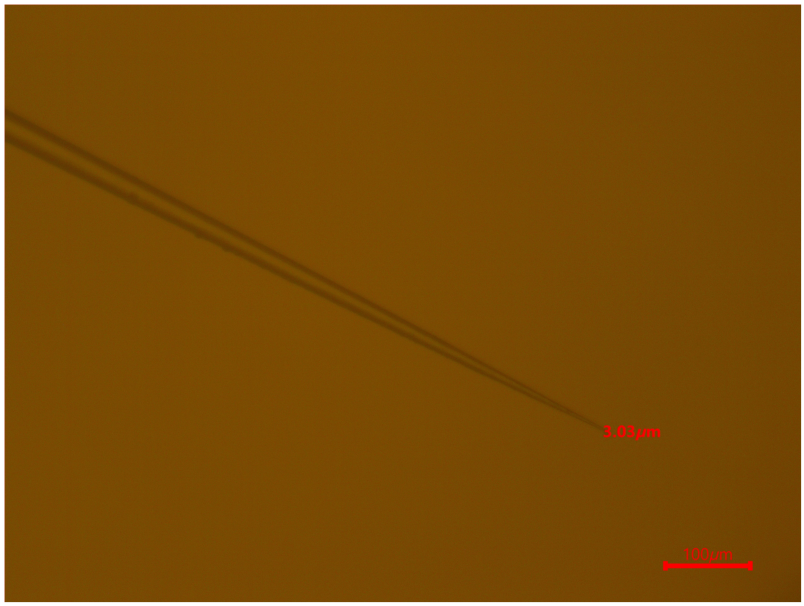

Fig. 4 Optical image of tapered fiber.

than does the core material,[22] which is also observed in Fig. 1. Therefore, as referenced in previous studies, a two-step etching process was selected.[22] It was observed that dipping the SMF in 30% of HF for about 90 min removed the majority of the cladding. Then, a diluted, 24% HF was used for precise control over the etch depth. An optical image of the obtained tapered fibre is shown in Fig. 4. Note that the pH of the container, strength of the HF, and humidity can affect the varying size of the diameter and the processing time.

The HF-acid vapor diffusion and the concentration gradient in the HF-air region aid in the fabricating of the tapered fiber. This occurs due to the slower etching of fiber at a lower concentration, which remains far from the fiber's end tip while a faster rate of fiber dissolution occurs toward the end tip. Silica is etched out by HF according to the following reaction:[23]

$$SiO_2 + 4HF \rightarrow SiF_4 + 2H_2O \quad (1)$$

$$SiO_2 + 6HF \rightarrow H_2SiF_6 + 2H_2O. \quad (2)$$

Both the reactions, according to Eqs. (1) and (2) occur at room temperature and under normal pressure; the first reaction dominates in a dehydrating medium or at a high HF concentration.[23] Upon exposure of the fiber to HF, the diameter of the fiber reduces (according to the reactions mentioned previously), which reduces the force from surface tension. During the process, the meniscus height reduces until the fiber is completely etched away leaving behind a conical tip.[22]

3.2 Characterization of Synthesized Au Nanoparticles and Their Functionalization on Fiber Probe

Figure 5(b) shows the UV-Vis absorption spectrum of the citrate-capped gold nanoparticles that are dispersed in DI water. During the synthesis, TNaC reduces Au(III) to Au. The Au NPs exhibit a strong absorption peak at 525 nm, which confirms localized surface plasmon resonance. From statistical analysis of the TEM images, as shown in Fig. 5(c), we find that the average size of the synthesized gold nanoparticles lies in the range of 16 nm.

Next, we characterize the gold nanoparticle-integrated tapered fibers. Figure 6(a) shows the SEM image of the tapered fiber. The diameter of the tapered fiber was found to be 3.5 μm with a taper angle of 3.3 deg. In Fig. 7, the SEM of the fiber shows the presence of gold nanoparticles. In Fig. 7(c), we see the elemental mapping results that confirm the Au NP coverage.

In Fig. 7, elements such as O, Si, S, Ge, and Au can be observed on the surface of the fiber. Because the core is doped with Ge, Ge is seen in the EDS. The atomic percentage of Au on the fiber is 0.12%, which is quite small in amount. This could result in less improvement in sensor performance. Despite the long-duration processing of the Au immobilization process, the low

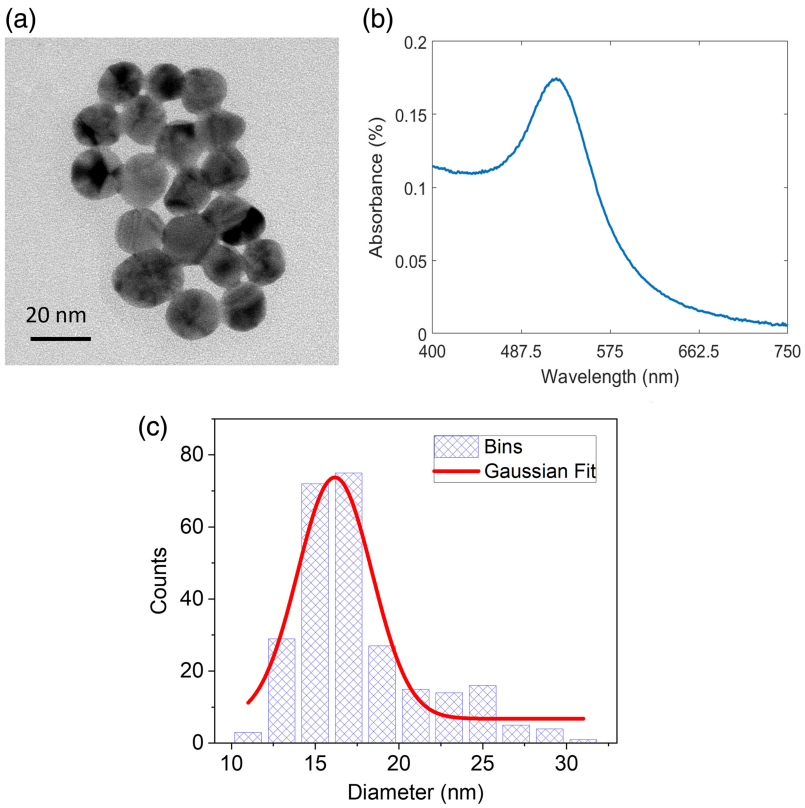

Fig. 5 Synthesized gold nanoparticles. (a) Transmission electron microscopy images. (b) UV-visible curve with resonance at 525 nm. (c) Histogram analysis of synthesized Au nanoparticles.

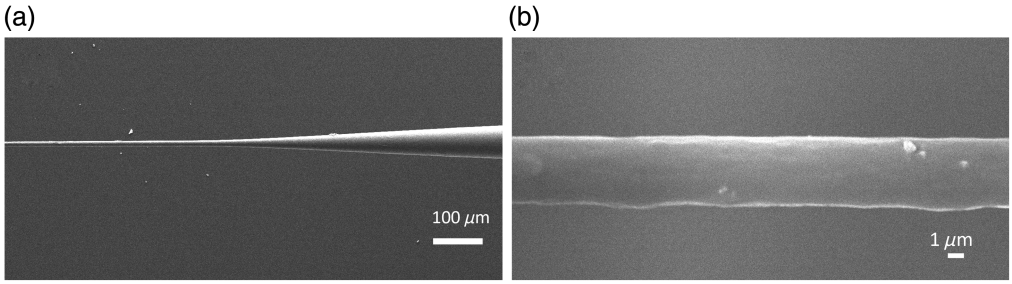

Fig 6 (a), (b) SEM of bare tapered optical fiber.

amount of gold nanoparticles could indicate that the size of the fiber plays an important role in the extent of gold immobilization. A diameter of 3.5 μm avails less surface area for gold functionalization. Therefore, although a smaller diameter may prove to be beneficial for maximum access to the evanescent field, in LSPR-based sensors, a smaller diameter may not be optimal. This is an important guiding principle for such plasmon-integrated tapered optical fiber sensors, which has not been discussed to date in the literature.

3.3 Refractive Index Sensing Performance

The refractive index for different sucrose concentrations is obtained using a Bellingham-Stanley OPTi Digital Handheld Refractometer, as shown in Fig. 8.

The work aims to study refractive index sensing when telecom fibers are used in the visible range. To obtain the data the central wavelength of the supercontinuum was chosen to be 525 nm with a bandwidth of 100 nm. The smoothened raw data (using a lowess function) obtained for both bare tapered fiber and gold-immobilized tapered fiber probe, in the reflection mode from the spectrometer is presented in Fig. 9. The raw data show that with immobilization of gold nanoparticles, there is some visible change in the spectrum otherwise obtained from the bare fiber.

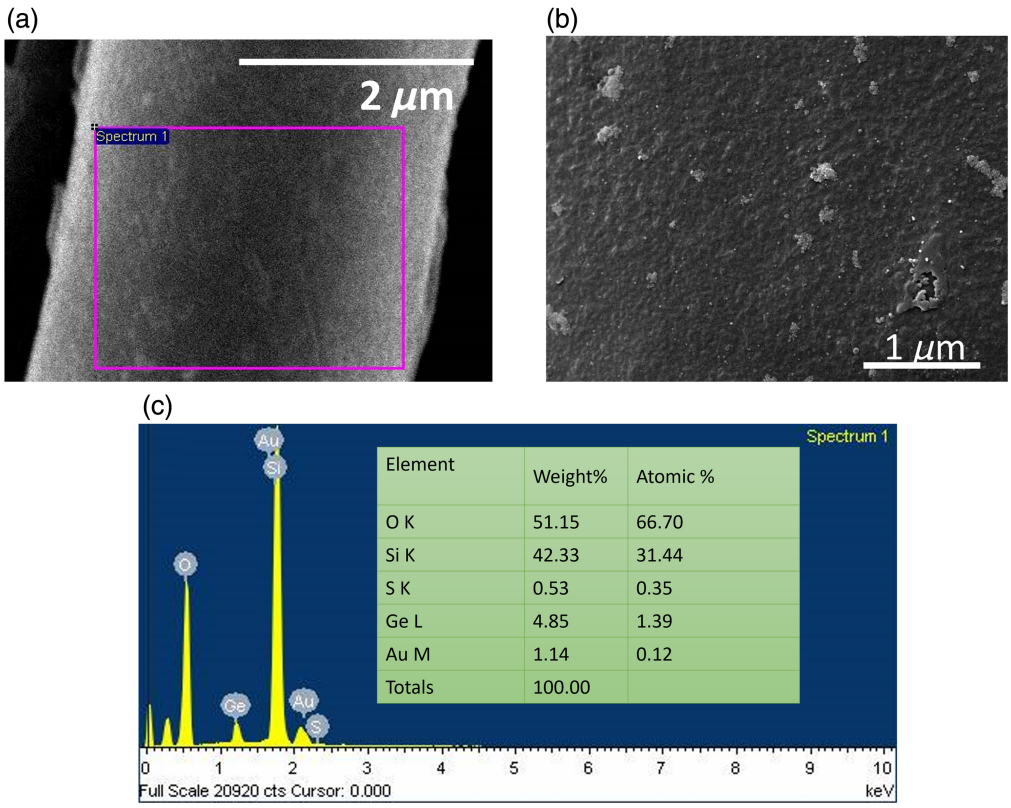

Fig. 7 (a), (b) Area of the Au-immobilized tapered fiber on which EDS is performed and (c) energy dispersive X-ray spectroscopy (EDS).

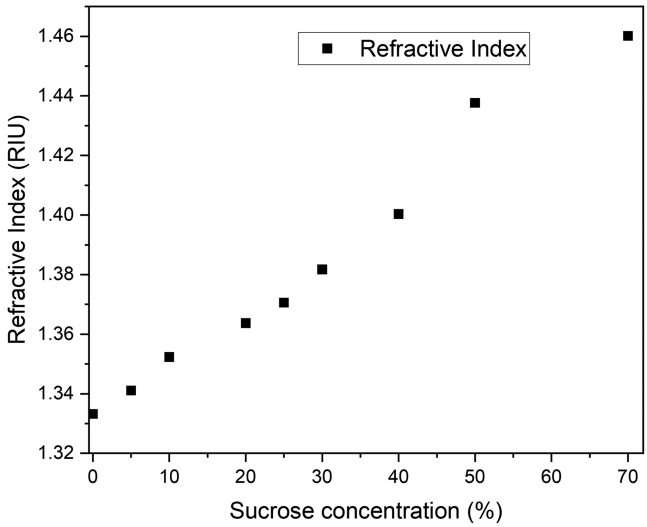

Fig. 8 Refractive index for different sucrose concentrations.

To understand the feature of gold nanoparticles on the fiber, normalization of the spectrum is undertaken. The normalized reflectance curve is shown in Fig. 10. The normalized curve is calculated as

$$R(\%) = \frac{I_{\mathrm{Au}}(n_{\mathrm{sucrose}})}{I_{\mathrm{bare}}(n = 1.33(0\%\text{sucrose concentration}))} * 100, \tag{3}$$

where I_{Au} is the intensity of the Au-immobilized fiber probe for different concentrations of sucrose solution and I_{bare} is the intensity of the bare tapered fiber probe at $n = 1.33$

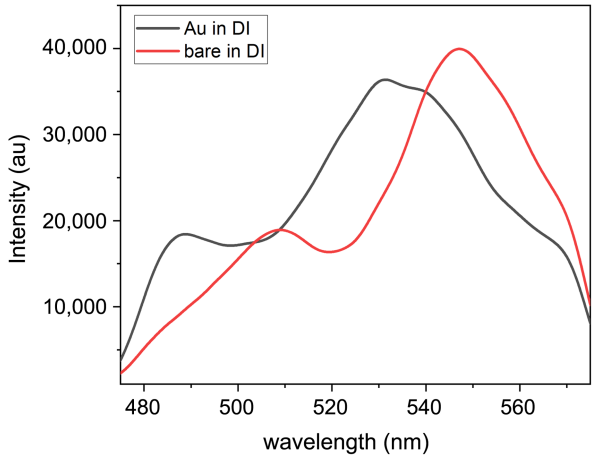

Fig. 9 Raw data for bare fiber (black) and gold immobilized fiber (red) probe when dipped in DI water.

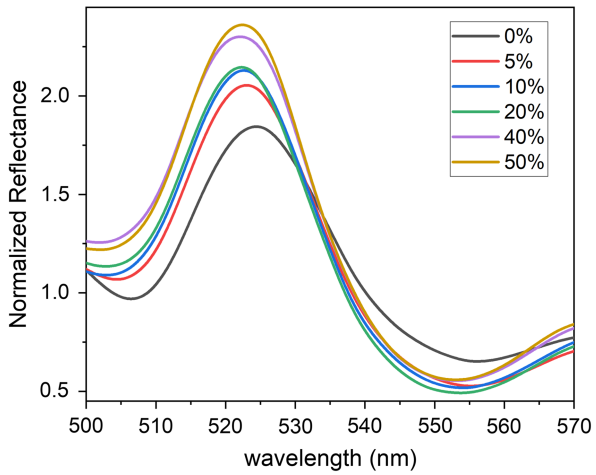

Fig. 10 Normalized reflectance data for Au-immobilized fibers.

corresponding to 0% sucrose solution. Therefore, using this equation, the intensity is analyzed for Au-immobilized fibers at resonance wavelength.

3.4 Performance of the Sensor Probe

3.4.1 *Sensitivity*

For an intensity-based sensor, we can define the sensitivity (S) of the normalized reflectance signal by[17]

$$S = \frac{\mathrm{dI}}{\mathrm{dn}}. \tag{4}$$

Using Eq. (4), the sensitivity curves are plotted and shown below in Fig. 11 for both intensity-based and wavelength-based sensor probes. Both the sensitivity plots show a linear response in the entire refractive index window. The sensitivity of the Au-immobilized fiber when used as a wavelength-based sensor probe is 15 nm/RIU. This is substantially higher than the resolution of the spectrometer. If the sensor is used as an intensity-based sensor probe, then the sensitivity is around 47,785.24 au/RIU.

The full-width at half-maximum (FWHM) for this sensor probe is found to be 23.96 nm. The quality factor (Q-factor) which is defined as the ratio of resonant wavelength to FWHM for the proposed sensor probe is calculated to be 22.93 when dipped in DI water. For a wavelength-based sensor, in comparison to the intensity-based sensor, rather than sensitivity function (S), the figure of merit (FOM) can offer a better picture of the performance characteristic.[24] The FOM is defined

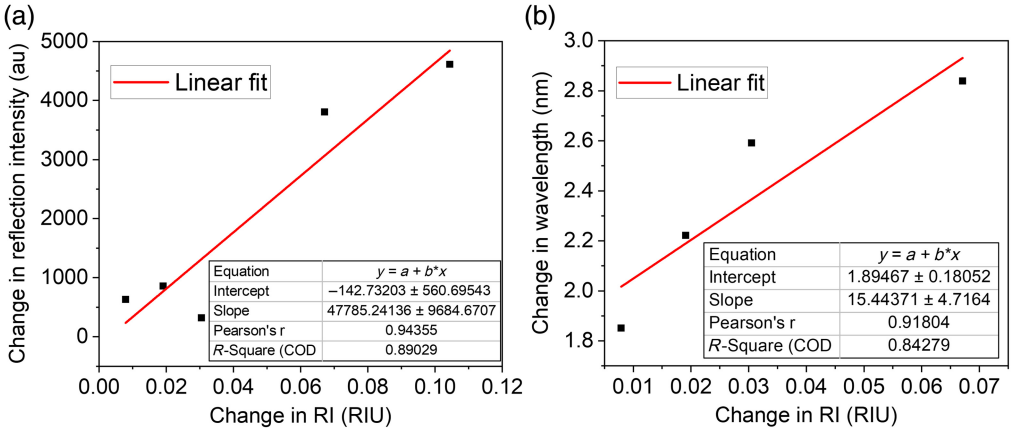

Fig. 11 Sensitivity curves for Au-immobilized tapered fiber when used as (a) intensity-based sensor probe and when used as (b) wavelength-based sensor probe.

as the ratio of sensitivity to FWHM. A reliable sensor should have minimum FWHM and high sensitivity which translates to a high FOM. For the proposed Au-immobilized sensor probe when dipped in DI, the FOM is calculated to be 0.674/RIU. Here, RIU is the refractive index unit.

3.5 Repeatability and Reliability

The repeatability and reliability of the sensor probes were also checked.

The reflectance intensity of two similar sensor probes shows similar results for 5% sucrose concentration, confirming the repeatability of the performance of the proposed sensor probes. To check the reliability of the sensor probes were tested for sucrose concentrations of 5% and 40%. The sensor probe was washed with DI, and then, the measurement was recaptured and plotted in Fig. 12. Therefore, the proposed sensor probe can be used for commercial purposes. Figure 12(b)

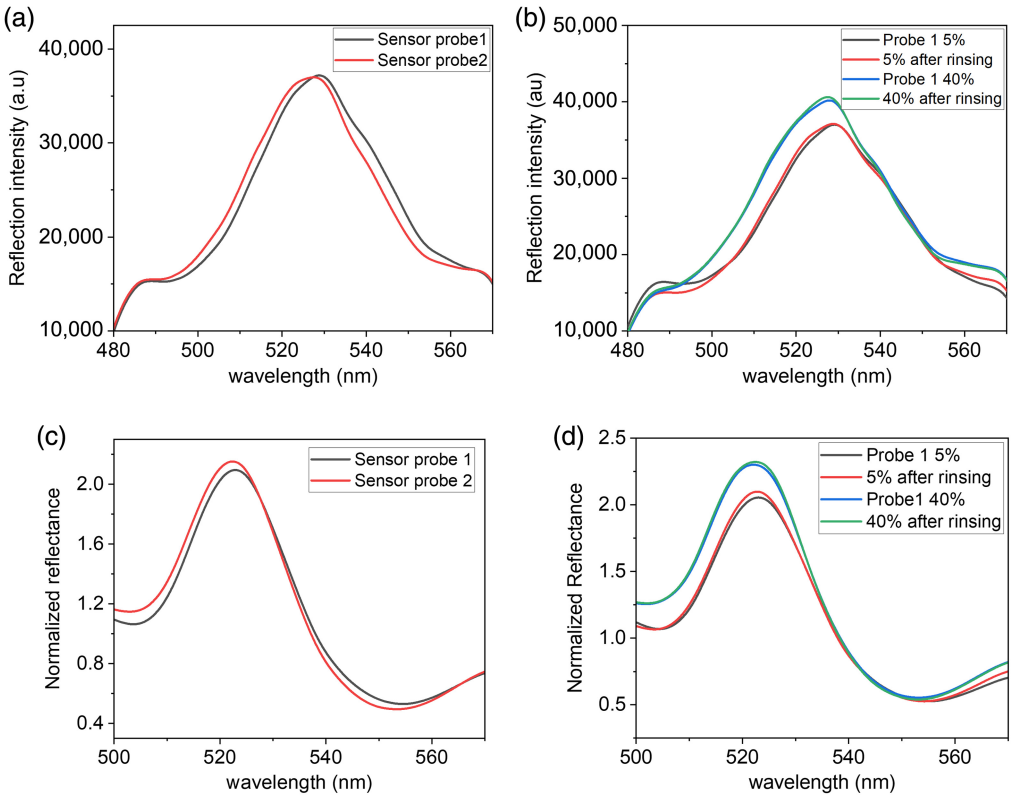

Fig. 12 (a) Repeatability test of two sensor probes for 5% sucrose concentration (b) Reliability of the sensor probe for 5% and 40% sucrose concentration. (c) Normalized repeatability test. (d) Normalized reliability test.

shows that the reflection spectra are similar in all the cases. In addition, the reflection intensity for the 40% sucrose solution is higher than the 5% sucrose solution.

4 Conclusion

A simple and low-cost method has been adopted to fabricate tapered telecommunication fiber probes using the HF chemical etching method. To achieve this, a two-step wet-etch process is used. In this process, first, the SMF is etched with 30% of HF acid for 90 min to remove a major portion of the cladding above the core. Subsequently, the SMF is etched using 24% of HF acid to decrease the core diameter; this is a slower process. A fiber diameter of 3.5 μm is obtained and used in the sensing experiment. Gold nanoparticles of an average diameter of between 16 and 24 nm are prepared by the Turkevich method and are immobilized on tapered fiber. The proposed Au-immobilized tapered telecommunication fiber probes are used to detect the refractive index change for a range of sucrose concentrations. The paper has also attempted to observe the suitability of this small-diameter telecommunication fiber as an intensity-based or wavelength-shift-based fiber. The widely available and cost-effective telecommunication fibers, immobilized with AuNPs when used with visible light can provide a performance of 15 nm/RIU as a wavelength-based sensor and 47, 785.24 au/RIU as an intensity-based sensor.

Disclosures

The authors declare that they have no potential conflicts of interest.

Code and Data Availability

All data in support of the findings of this paper are available within the article.

Acknowledgments

The authors acknowledge the Laboratory of Optics of Quantum Materials Laboratory, Physics Department, IIT Bombay, for providing the optical experiment facility, Sophisticated Analytical Instrument Facility (SAIF); the Centre for Research in Nanotechnology and Science (CRNTS), IIT Bombay, for providing sample characterization facilities, the Centre of Excellence Nanoelectronics (CEN), IIT Bombay, for providing the sample preparation facility, and the Department of Bio-Technology, India, for funding the project.

References

1. J. M. Senior and M. Y. Jamro, *Optical Fiber Communications: Principles and Practice*, Pearson Education (2009).
2. L. Bo, "Tapered optical microfibre based structures for sensing applications," PhD, School of Electronics and Communication Engineering, Dublin Institute of Technology, pp. 8–29 (2015).
3. B. Guzowski and M. Łakomski, "Temperature sensor based on periodically tapered optical fibers," *Sensors* **21**(24), 8358 (2021).
4. X. Lei, Y. Feng, and X. Dong, "High-temperature sensor based on a special thin-diameter fiber," *Opt. Commun.* **463**, 125386 (2020).
5. Y. Wang et al., "Water pollutants p-cresol detection based on Au-ZnO nanoparticles modified tapered optical fiber," *IEEE Trans. Nanobiosci.* **20**(3), 377–384 (2021).
6. S. Wang et al., "Simultaneous measurement of the BOD concentration and temperature based on a tapered microfiber for water pollution monitoring," *Appl. Opt.* **59**(24), 7364–7370 (2020).
7. Y. Wang et al., "Transformer oil-dissolved methane detection based on non-adiabatic tapered fiber using polyacrylate and cryptophane–a overlay deposition," *Sens. Actuators B: Chem.* **400**, 134869 (2024).
8. M. M. Alkhabet et al., "Room temperature operated hydrogen sensor using palladium coated on tapered optical fiber," *Mater. Sci. Eng. B* **287**, 116092 (2023).
9. T. Dong et al., "Label-free tapered fiber optic sensor for real-time in situ detection of cell activity," *IEEE Sens. J.* **23**, 15622–15627 (2023).
10. N. Mar-Abundis et al., "Sugar detection in aqueous solution using an SMS fiber device," *Sensors* **23**(14), 6289 (2023).
11. M. Aziz et al., "Glucose oxidase-based enzyme immobilised on tapered optical fibre for reliability improvement in selective glucose sensing," *Optik* **259**, 168970 (2022).

12. E. Multar et al., "Functionalized fiber optics for glucose detection," *J. Phys.: Conf. Ser.* **1484**(1), 012010 (2020).
13. P. Zaca-Morán et al., "Etched optical fiber for measuring concentration and refractive index of sucrose solutions by evanescent waves," *Laser Phys.* **28**(11), 116002 (2018).
14. A. J. Rodriguez et al., "Optical fiber sensors based on nanostructured materials for environmental applications," PhD dissertation, Universidad Publica de Navarra (2014).
15. C.-H. Huang et al., "The phase-response effect of size-dependent optical enhancement in a single nanoparticle," *Opt. Express* **16**(13), 9580–9586 (2008).
16. K. M. Mayer and J. H. Hafner, "Localized surface plasmon resonance sensors," *Chem. Rev.* **111**(6), 3828–3857 (2011).
17. H.-Y. Lin et al., "Tapered optical fiber sensor based on localized surface plasmon resonance," *Opt. Express* **20**(19), 21693–21701 (2012).
18. J. Kimling et al., "Turkevich method for gold nanoparticle synthesis revisited," *J. Phys. Chem. B* **110**, 15700–15707 (2006).
19. C. Beatrice et al., "Surfactant-mediated desorption of polymer from the nanoparticle interface," *Langmuir* **28**(5), 2485–2492 (2012).
20. X. Yang et al., "Silicon wafer wettability and aging behaviors: impact on gold thin-film morphology," *Mater. Sci. Semicond. Process.* **26**, 25–32 (2014).
21. J. Satija et al., "Optimal design for U-bent fiber-optic LSPR sensor probes," *Plasmonics* **9**, 251–260 (2014).
22. H. J. Kbashi, "Fabrication of submicron-diameter and taper fibers using chemical etching," *J. Mater. Sci. Technol.* **28**(4), 308–312 (2012).
23. Y. Zaatar et al., "Fabrication and characterization of an evanescent wave fiber optic sensor for air pollution control," *Mater. Sci. Eng. B* **74**(1), 296–298 (2000).
24. J.-T. Lin et al., "Analysis of scaling law and figure of merit of fiber-based biosensor," *J. Nanomater.* **2012**, 3 (2012).

Debanita Das is currently pursuing her PhD from IITB-Monash Research Academy. Her current research interest is to explore the properties of fibre optics coupled with noble metals to improve the performance of sensors. She received her BTech degree in electrical engineering from Tezpur Central University, India in 2019 and MTech degree in green energy technology from Pondicherry Central University, India in 2021. She is a member of SPIE.

Biographies of the other authors are not available.